11. D. Pietrobon, B. Prod'hom, P. Hess, *Nature* **333**, 373 (1988).
12. X. C. Yang and F. Sachs, *Biophys. J.* **53**, 412a (1988).
13. J. B. Lansman, T. Hallam, T. J. Rink, *Nature* **325**, 811 (1987).
14. M. T. Kirber, J. J. Singer, J. V. Walsh, *Biophys. J.* **51**, 252a (1987).
15. J. A. Dani, *ibid.* **49**, 607 (1986).
16. R. W. Tsien, P. Hess, E. W. McCleskey, R. L. Rosenberg, *Annu. Rev. Biophys. Biophys. Chem.* **16**, 265 (1988).
17. C. Methfessel *et al.*, *Pfluegers Arch.* **407**, 577 (1986).
18. M. T. Kirber, J. V. Walsh, Jr., J. J. Singer, *Biophys. J.* **53**, 411a (1988).
19. W. J. Sigurdson, C. E. Morris, B. L. Brezden, D. R. Gardner, *J. Exp. Biol.* **127**, 191 (1987).
20. C. Chen, M. J. Corbley, T. M. Roberts, P. Hess, *Science* **239**, 1024 (1988).
21. O. A. Krishtal, V. I. Pidoplichko, Y. A. Shakhovalov, *J. Physiol. (London)* **310**, 423 (1981).
22. F. Guharay and F. Sachs, *ibid.* **353**, 119 (1985).
23. J. P. Ding, personal communication.
24. M. C. Gustin, X.-L. Zhou, B. Martinac, M. R. Culbertson, C. Kung, *Biophys. J.* **51**, 251a (1987).
25. M. C. Gustin, X.-L. Zhou, B. Martinac, C. Kung, *Science* **242**, 762 (1988).
26. C. Deutsch and S. C. Lee, *Renal Physiol.*, in press.
27. R. J. Docherty, *J. Physiol. (London)* **398**, 33 (1988).
28. O. P. Hamill, A. Marty, E. Neher, B. Sakmann, F. J. Sigworth, *Pfluegers Arch.* **391**, 85 (1981).
29. A. Auerbach and F. Sachs, *Biophys. J.* **45**, 187 (1984).
30. F. Guharay and F. Sachs, *J. Physiol. (London)* **352**, 685 (1984).
31. F. Sachs, *Membrane Biochem.* **6**, 173 (1986).
32. ———, J. Neil, N. Barkakati, *Pfluegers Arch.* **395**, 331 (1982).
33. Z. Xiang, J. Neil, A. Auerbach, *P. R. Health Sci. J.* **7** (2), 77 (1988).
34. E. Neher, *J. Physiol. (London)* **339**, 663 (1983).
35. B. Hille, *Ionic Channels of Excitable Membranes* (Sinauer, Sunderland, MA, 1984).
36. We thank J. P. Ding for providing unpublished results. A preliminary report on these results was presented at the 1988 Biophysical Society Meeting (*12*). Supported by the Muscular Dystrophy Association, USARO 22560-LS, NIH DK-37792, and the Health-care Instruments and Devices Institute at the State University of New York at Buffalo.

4 August 1988; accepted 2 December 1988

Neuroanatomical Correlates of Anticipatory Anxiety

ERIC M. REIMAN, MAUREEN J. FUSSELMAN, PETER T. FOX, MARCUS E. RAICHLE

Positron emission tomographic measurements of regional blood flow, a marker of local neuronal activity, were used to investigate the neuroanatomical correlates of a normal emotion. Healthy volunteers were studied before, during, and after anticipation of a painful electric shock. During anticipatory anxiety, there were significant blood flow increases in bilateral temporal poles, the same regions recently implicated in a lactate-induced anxiety attack in patients with panic disorder. Thus, the temporal poles seem to be involved in normal and pathological forms of human anxiety.

IN ORDER TO ESTABLISH THE NEUROBIology of an emotional response, researchers must be able to relate that response to the local processes of the living human brain. Previously, we used positron emission tomography (PET) to investigate the neuroanatomical correlates of panic disorder, a pathological form of human anxiety (*1–3*). Patients with panic disorder and normal control subjects were studied before and during lactate infusion, a procedure that precipitated an anxiety attack in many of the patients and none of the controls (*2, 3*). During the nonpanic state before the infusion, the patients who were vulnerable to lactate-induced panic had an abnormal asymmetry (left less than right) of blood flow, of blood volume, and of the metabolic rate for oxygen in the vicinity of Economo's region TH in the parahippocampal gyrus (*2*). During a lactate-induced anxiety attack, there were significant blood flow increases in bilateral regions of the temporal poles (*3*).

In the study reported here, we used PET measurements of regional blood flow, a marker of local neuronal activity (*4*), to investigate the neuroanatomical correlates of a normal form of human anxiety, that due to the anticipation of an external danger. Regional blood flow was measured in eight healthy volunteers (*5*) before, during, and after anticipation of a painful electric shock. These measurements were made with the PETT VI system, [^{15}O]H_2O, 40-s data acquisition periods, and an interscan duration of 10 min (*6, 7*). The subjects were informed that no shock would be delivered during the first and third measurements, but that a painful electric shock would be delivered sometime within a 2-min period after the second tracer administration; they were also informed that the severity of the shock was likely to increase with the passage of time before its arrival. A brief electric shock was delivered immediately after the second data acquisition period to maintain the credibility of the investigators for the remainder of the study; the severity of the stimulus was predetermined by its ability to produce mild discomfort in the investigators themselves (*8*).

The first scanning procedure permitted acclimation to the PET routine and provided data for post hoc comparisons. The second scanning procedure provided data corresponding to a state of anticipatory anxiety. The third scanning procedure provided baseline data for measuring the changes in

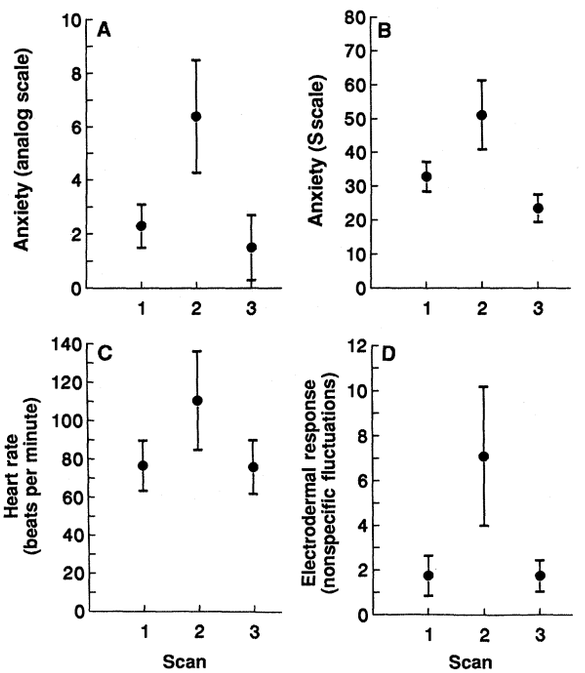

Fig. 1. Subjective and physiologic measurements of anxiety before (scan 1), during (scan 2), and after (scan 3) anticipation of a painful electric shock. Means and standard deviations are depicted for (**A**) the rating on an analog scale of anxiety, (**B**) the score on the S-Anxiety scale of the STAI (*10*), (**C**) heart rate, and (**D**) the number of nonspecific fluctuations in skin conductance. Scan 2 was distinguished from scans 1 and 3 by significant increases in all measures of anxiety (paired t tests, $P < 0.05$, Bonferroni correction for multiple comparisons).

E. M. Reiman, Department of Psychiatry and McDonnell Center for Studies of Higher Brain Function, Washington University School of Medicine, St. Louis, MO 63110.
M. J. Fusselman, Departments of Psychiatry and Neurology and Neurological Surgery, Washington University School of Medicine, St. Louis, MO 63110.
P. T. Fox, Mallinckrodt Institute of Radiology and Department of Neurology and Neurological Surgery, Washington University School of Medicine, St. Louis, MO 63110.
M. E. Raichle, Mallinckrodt Institute of Radiology, Department of Neurology and Neurological Surgery, and McDonnell Center for Studies of Higher Brain Function, Washington University School of Medicine, St. Louis, MO 63110.

regional blood flow related to anticipatory anxiety. After completion of the first three scans, four subjects had three additional scans to determine if the regional blood flow increases associated with the production of anxiety might be related to voluntary movements or increased motor tone independent of the anxious state (*9*).

An analog scale and the S-Anxiety scale of the State-Trait Anxiety Inventory (STAI) were used to assess the subjective state of anxiety related to each scan (*10*). Heart rate and electrodermal activity, physiologic variables known to reflect an individual's state of anxiety (*11*), were recorded during each scan. An automated technique for the analysis of PET data was used to identify the changes in regional blood flow associated with anticipatory anxiety (*12*).

During anticipation of the shock, there were significant increases in the subjective and physiological measurements of anxiety (Fig. 1) (*13*); every subject exhibited increases in each of these measurements. During anticipatory anxiety, there were significant increases in regional blood flow ($G2 = 2.89$, $P < 0.01$), but no significant decreases ($G2 = 1.33$, $P > 0.05$).

The significant blood flow increases were located in bilateral temporal poles (Table 1 and Fig. 2), the same regions that we previously implicated in a lactate-induced anxiety attack (*3, 14*). Post hoc analyses supported the consistency of these increases (paired *t* tests, $P < 0.05$) (*15*). The vertical extent of the blood flow increases greatly exceeded the transverse resolution of the image (Fig. 2), suggesting the presence of additional blood flow increases in bilateral temporofrontal regions near the anterior aspect of the lateral sulcus. The increases in temporopolar blood flow appear to be unrelated to scan order (*16*), anticipation (*17, 18*), voluntary movements (*19*), or increased motor tone (*19*) independent of the anxious state.

We have demonstrated involvement of the temporal poles in pathological and normal forms of human anxiety. Our findings are compatible with stimulation and lesion studies. Temporopolar stimulation influences the autonomic functions often associated with the anxious state (*20*); it produces a syndrome in nonhuman primates characterized by behavioral inhibition, apparent hypervigilance, and altered facial expressions seeming to reflect "arousal, attention, or anxiety" (*20*); and it produces the experience of fear in patients with temporal lobe epilepsy (*21*). Bilateral lesions of temporopolar cortex in nonhuman primates attenuate the expressions of fear in response to normally threatening situations (*22*). Fear is commonly experienced in association with temporal lobe seizures (*21, 23*), and anxiety attacks

Table 1. Location and *z* score of the significant mean increases in regional blood flow associated with the production of anticipatory anxiety. These data correspond to the image of mean increases in regional blood flow shown in Fig. 2. *X*, *Y*, and *Z* are spatial coordinates with respect to a point in a horizontal plane through the anterior and posterior commissures ($Z = 0$), at the midline of the horizontal brain slice ($X = 0$), and at the midpoint between the anterior and posterior commissures ($Y = 0$). *X* is the distance to the left (positive) or right (negative) of the midline. *Y* is the distance anterior (positive) or posterior (negative) to the midpoint between the anterior and posterior commissures. *Z* is the distance above (positive) or below (negative) a horizontal plane through the anterior and posterior commissures. The spatial coordinates correspond to those from specimen VF 25 (*27*). Each *z* score was calculated as the magnitude of the mean increase in regional blood flow divided by the standard deviation of all regional blood flow increases associated with the production of anticipatory anxiety.

Identified region	Location (mm)			*z* score
	X	*Y*	*Z*	
Temporopolar cortex (right)	−54	+28	−26	4.4*
Temporopolar cortex (left)	+49	+30	−24	4.1*

*$P<0.00005$ (before Bonferroni correction).

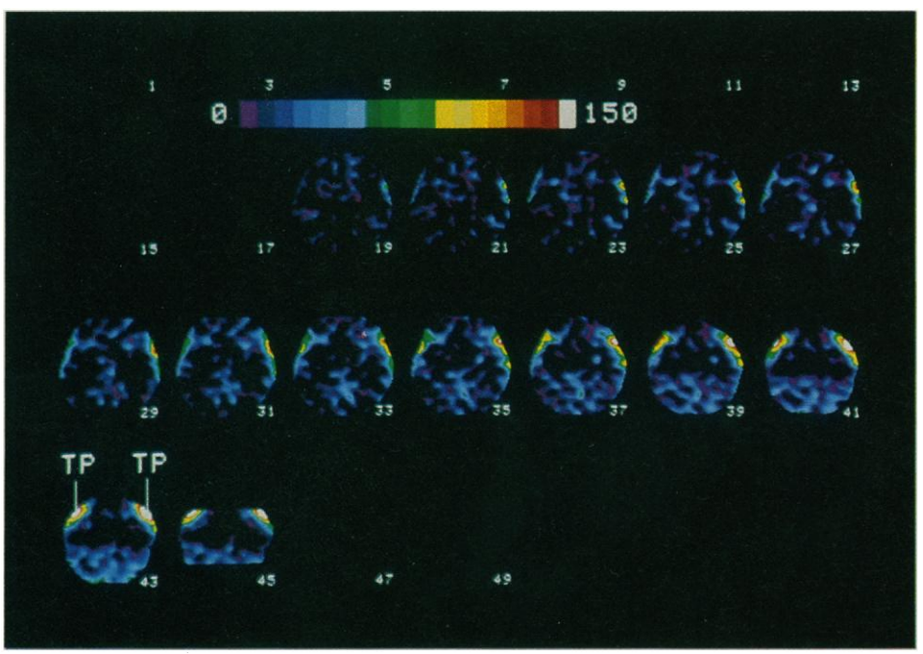

Fig. 2. The image of mean increases in regional blood flow associated with the production of anticipatory anxiety. All brain sections are parallel to a horizontal plane through the anterior and posterior commissures (slice 31). The right hemisphere in each image is on the reader's right. The centers of contiguous slices are 2 mm apart, but only odd-numbered planes are shown. The color scale is linear and in units of PET counts per pixel per scan (*7*). The production of anticipatory anxiety was associated with significant blood flow increases in bilateral temporal poles (TP).

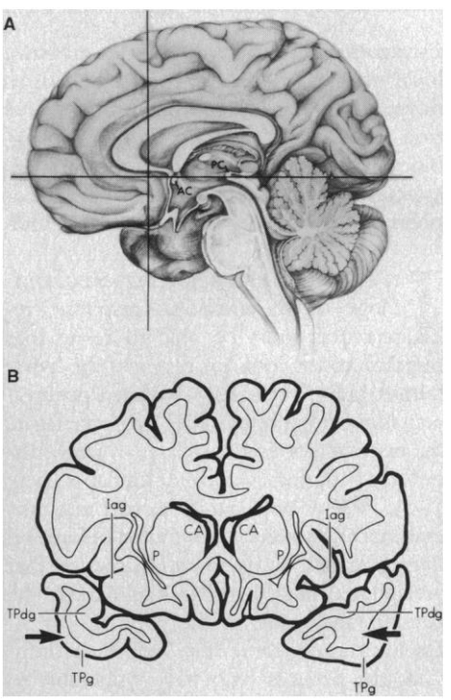

Fig. 3. (**A**) An illustration of the medial surface of a bisected brain. The horizontal line represents a plane through the anterior commissure (AC) and posterior commissure (PC). The vertical line indicates the plane of (**B**), a verticofrontal section through the temporal poles. The right hemisphere in (B) is on the reader's left. The arrows indicate the sites of maximal blood flow increases. The anatomical localization procedure used to identify these blood flow increases has an SD of about 5 mm in each axis (*12*). Abbreviations: TPg, granular region of temporopolar cortex; TPdg, dysgranular region of temporopolar cortex; Iag, agranular region of insular cortex; CA, caudate; and P, putamen.

sometimes develop in association with anterior temporal lobe pathology (*24*).

Because of its anatomical connections with sensory association areas and the amygdala, Mesulam and his colleagues (*25*) refer to temporopolar cortex as a "paralimbic area." They suggest that temporopolar cortex evaluates the relevance of environmental information, leading to the production of an appropriate response (*25*). In regard to anxiety, the temporal poles could be involved in the evaluation process that characterizes a situation with a sense of uncertainty, helplessness, or danger.

Panic disorder appears to be distinguished from normal forms of anxiety by the presence of a regional brain abnormality in the nonpanic state, an abnormality that could be involved in the initiation of an anxiety attack (*2, 26*). However, lactate-induced panic and normal anticipatory anxiety appear to share a common pathway involving the temporal poles.

REFERENCES AND NOTES

1. Committee on Nomenclature and Statistics, *Diagnostic and Statistical Manual of Mental Disorders* (American Psychiatric Association, Washington, DC, rev. ed. 3, 1987); E. M. Reiman, *Psychiatr. Dev.* **1**, 63 (1987).
2. E. M. Reiman, M. E. Raichle, F. K. Butler, P. Herscovitch, E. Robins, *Nature* **310**, 683 (1984); E. M. Reiman *et al.*, *Am. J. Psychiatry* **143**, 469 (1986).
3. Smaller but significant blood flow increases were also identified bilaterally in insular cortex, claustrum, or lateral putamen, in the vicinity of the superior colliculus; and in the vicinity of the left anterior cerebellar vermis (E. M. Reiman *et al.*, *New Research Abstracts*, annual meeting of the American Psychiatric Association, Montreal, Canada, May 1988, p. 26).
4. M. E. Raichle, *Handbook of Physiology, The Nervous System*, vol. 5, *Higher Functions of the Brain*, F. Plum, Ed. (American Physiological Society, Bethesda, MD, 1987), pp. 643–674.
5. The subjects denied a history of psychiatric, neurologic, or other medical disorders. Absence of psychiatric disorders was confirmed with a structured interview [R. L. Spitzer and J. B. W. Williams, *Structured Clinical Interview for DSM-III—Upjohn Version* (New York State Psychiatry Institute, New York, 1983)]. The subjects were informed that the purpose of the study was to establish the physiologic response to the prospect of a painful stimulus. The consent form stated that only one shock would be delivered during the study, that the shock would be delivered within 2 min after the tracer administration, and that it was likely to be painful. Subjects were informed that they could withdraw from the study at any time. Informed consent was obtained in accordance with guidelines approved by the Human Studies Committee and the Radioactive Drug Research Committee (Food and Drug Administration) of Washington University. Subject preparation included the use of a thermally molded facial mask to minimize head movements during the study; a lateral skull radiograph to ensure sampling of the inferior temporal lobes and record the relation between each PET slice and the cranial landmarks; a catheter in the right antecubital vein to permit tracer administration; bilateral leads adjacent to the lateral canthus to record extraocular movements; leads on the wrists to record heart rate; leads on the index fingers to record electrodermal activity; and conical sleeves over the fourth finger of each hand to permit delivery of the electric shock. During each scan, the subjects rested quietly in the supine position with eyes closed, with undetectable movements of the eyes or limbs, and without sensory stimulation.
6. M. M. Ter-Pogossian *et al.*, *J. Comput. Assist. Tomogr.* 6, 125 (1982); M. Yamamoto, D. C. Ficke, M. M. Ter-Pogossian, *IEEE Trans. Nucl. Sci.* **29**, 529 (1982).
7. The images were analyzed in units of PET counts per pixel per scan rather than in milliliters per minute per 100 g to eliminate the need for arterial catheterization and the possibility that this procedure might have a confounding effect on the anxious response. There is a nearly linear relation between regional measurements of PET counts and blood flow when the data are acquired for 40 s after the intravenous bolus injection of $[^{15}O]H_2O$ [P. Herscovitch, J. Markham, M. E. Raichle, *J. Nucl. Med.* **14**, 782 (1983); P. T. Fox *et al.*, *J. Cereb. Blood Flow Metab.* **4**, 329 (1984)]. Measurements of regional PET counts and regional blood flow are associated with virtually identical sensitivity and specificity in the detection of state-dependent responses, although the magnitude of the tissue activity response is slightly smaller (P. T. Fox and M. A. Mintun, *J. Nucl. Med.*, in press).
8. The electric stimulus was delivered for 3 s with a Grass S88 stimulator and a Grass stimulus isolation unit. It produced a tingling sensation or mild discomfort in the exposed fingers. After the stimulus, the subjects reported that the shock was less unpleasant than they expected; they expressed relief that the prospect of the shock had passed.
9. During the fourth scan, these four subjects opened and closed their right fist approximately once per second. During the fifth scan, they rested without movements; this scan served as the control for the fourth and sixth scans. During the sixth scan, the subjects maintained tonic contraction of the right hand in the form of a fist.
10. Immediately after each scan, the subjects were asked to rate their experience of "anxiety or emotional discomfort during the scan" on a scale of 0 to 10. They were also asked to rate 20 items from the S-Anxiety scale pertaining to their anxiety during the scan; possible scores on this scale range from 20 to 80 [C. D. Spielberger, *Manual for the State-Trait Anxiety (STAI Form Y)* (Consulting Psychologists Press, Palo Alto, CA, 1983)].
11. G. Deane, *J. Exp. Psychol.* **61**, 489 (1961); R. Elliott, *J. Pers. Soc. Psychol.* **3**, 353 (1965); M. Lader, *Handbook of Studies on Anxiety*, G. D. Burrows and B. Davies, Eds. (Elsevier, New York, 1981), pp. 59–88.
12. P. T. Fox, M. A. Mintun, E. M. Reiman, M. E. Raichle, *J. Cereb. Blood Flow Metab.* **8**, 642 (1988); also see (*7*). Each PET image consisted of seven horizontal slices with an in-plane resolution of 12.4 to 14.7 mm, a transverse resolution of 9.7 to 20.5 mm, and an interslice distance of 14.4 mm. First, each image was normalized to a mean of 1000 counts by multiplying every pixel in the image by the same linear correction factor. Second, an image of regional blood flow changes was computed in each subject as the pixel by pixel subtraction of the control image (the third scan) from the experimental image (the second scan). Third, a linear interpolation was performed on each seven-slice image of blood flow changes to generate data for voxels existing between the imaged planes (M. A. Mintun, P. T. Fox, M. E. Raichle, *J. Cereb. Blood Flow Metab.*, in press). Fourth, a computer algorithm for anatomical localization [P. T. Fox, J. W. Perlmutter, M. E. Raichle, *J. Comput. Assist. Tomogr.* **9**, 141 (1985)] was used to transform each interpolated image of blood flow changes into a stereotactically standardized data matrix. Fifth, the spatially standardized images of blood flow changes were averaged on a voxel by voxel basis. Data located outside the volume between the uppermost and lowermost slices of any of the individual, stereotactically standardized images were excluded from the averaged image. This procedure produced an image of mean changes in regional blood flow related to anticipatory anxiety (Fig. 2). (Although a template was used to exclude data outside the brain in the creation of Fig. 2, it was not used in the data analysis procedure.) An automated program computed the magnitude and stereotactic location of all maxima and minima in the image of blood flow changes. State-dependent regional changes, defined as significant "outliers" in the distribution of mostly random blood flow changes, were established by computation of the gamma-2 statistic (G2) from the population of regional blood flow changes. A significantly positive G2 is specific for populations that contain nonrandom changes in regional blood flow. To test independently for state-dependent increases and decreases in regional blood flow, a one-sided G2 was computed for the values on each side of the mean of the population of changes, which was close to zero. For populations characterized by a significantly positive G2, z scores (response magnitude divided by standard deviation) were used to characterize the nonrandom changes in regional blood flow. Significant blood flow changes were defined on the basis of a z score ≥ 1.65, which has a cumulative normal probability >0.95. Because populations of random blood flow change are clustered closer to the mean than a normal population, estimates of cumulative probability from tables that assume normality are conservative. For regions with a significant mean blood flow change, individual changes in blood flow were computed from each set of paired images. A paired t test was performed on these intrasubject changes in regional blood flow to assess their consistency. In addition, a paired t test was performed to compare the left-to-right ratio of blood flow in parahippocampal region TH during the second and third scans. This analysis determined whether the abnormal parahippocampal asymmetry found in patients who were vulnerable to lactate-induced panic (*2*) could have reflected a state of anticipatory anxiety.
13. Increases in these physiologic measurements persisted and typically increased throughout the second 40-s scan.
14. The relation between the increases in temporopolar blood flow and anxiety is supported by the significant G2 statistic, the magnitude of the z scores (Table 1; $P < 0.01$, after Bonferroni correction for multiple comparisons), the bilaterality of the blood flow increases, the consistency of these increases among individual subjects, the reproducibility of our findings with either the first or third scan as the control, and the reproducibility of our findings with two distinct anxiogenic procedures (that is, lactate infusion and anticipation of shock) (*3, 15, 16*). No other significant changes in regional blood flow were found. However, negative findings could be attributable to limitations in spatial resolution and anatomical standardization, the conservative nature of our data analysis procedure, and the relatively small number of subjects in this study.
15. Every subject exhibited a blood flow increase in at least one of the temporal poles. Seven subjects had an increase in the right temporopolar region and seven subjects had an increase in the left. The mean ± SD of the blood flow increases was 103 ± 93 counts in the right temporal pole and 69 ± 55 counts in the left temporal pole. The difference between the left and right temporopolar blood flow increases failed to reach significance (paired t test, $P = 0.27$), even when the analysis was restricted to the right-handed subjects ($P = 0.35$).
16. Anticipatory anxiety was associated with significant increases in temporopolar blood flow even when the first scan was used as the control (G2 = 2.87, z scores = 4.3 in the right and 4.0 in the left temporal pole).
17. There were no significant differences in regional blood flow between the first and third scans (G2 statistics, $P > 0.05$). Thus, the increases in temporopolar blood flow were unrelated to anticipation of a novel situation (that is, the first PET scan) in the absence of severe anxiety.
18. In a separate study, anticipation of an emotionally neutral visual cue was not associated with significant increases in temporopolar blood flow (J. Pardo, personal communication).
19. There were no significant changes in regional blood flow associated with movements or increased motor tone in the right hand (G2 statistics, $P > 0.05$). (Primary motor cortex and the supplementary motor area were located superior to the uppermost PET slice in the averaged image.) When analysis of scans two and three was restricted to the four subjects who

had the additional scans, there were still significant increases in temporopolar blood during the production of anticipatory anxiety.
20. B. R. Kaada, *Handbook of Physiology*, Section 1, *Neurophysiology*, J. Field and H. W. Magoun, Eds. (American Physiological Society, Washington, DC, 1960), vol. 2, pp. 1345–1372.
21. W. Penfield and H. Jasper, *Epilepsy and the Functional Anatomy of the Human Brain* (Little, Brown, Boston, 1954).
22. A. Kling and H. D. Steklin, *Brain Behav. Evol.* **13**, 216 (1976).
23. E. Halgren and R. Walter, *Brain* **101**, 83 (1978); P. Gloor, A. Olivier, L. F. Quesney, F. Andermann, S. Horowitz, *Ann. Neurol.* **12**, 129 (1982); E. Strauss, A. Risser, M. W. Jones, *Arch. Neurol.* **39**, 626 (1982).
24. M. Wall *et al.*, *J. Clin. Psychiatry* **46**, 143 (1985); M. Wall, D. Mielke, J. S. Luther, *ibid.* **47**, 219 (1986); A. M. Ghadirian *et al.*, *ibid.*, p. 270.
25. M. M. Mesulam and E. J. Mufson, *J. Comp. Neurol.* **212**, 1 (1982); M. A. Moran, E. J. Mufson, M. M. Mesulam, *ibid.*, **256**, 88 (1987).
26. There was no significant difference between the left-to-right ratio of parahippocampal blood in the second and third scans ($P = 0.97$). Thus, the abnormal parahippocampal asymmetry in patients with panic disorder seems to be unrelated to a state of anticipatory anxiety.
27. J. Talairach and G. Szikla, *Atlas d'Anatomie Stereotaxique du Telencephale* (Masson, Paris, 1967).
28. We thank J. Stern and J. Price for helpful suggestions, L. Lich for technical support, and S. Sirkin and J. Woodward for secretarial assistance. Supported by National Institute of Mental Health Physician Scientist Award MH-00615 (E.M.R.); National Institute of Neurological and Communicative Disorders and Stroke (NINCDS) Teacher Investigator Award NS-00904 (P.T.F.); NINCDS grant NS-06833; National Heart, Lung, and Blood Institute grant HL-13851; and a grant from the Upjohn company.

29 August 1988; accepted 11 November 1988

Structure and Function of Human Amphiregulin: A Member of the Epidermal Growth Factor Family

MOHAMMED SHOYAB, GREGORY D. PLOWMAN, VICKI L. MCDONALD, J. GARRETT BRADLEY, GEORGE J. TODARO

The complete amino acid sequence of amphiregulin, a bifunctional cell growth modulator, was determined. The truncated form contains 78 amino acids, whereas a larger form of amphiregulin contains six additional amino acids at the amino-terminal end. The amino-terminal half of amphiregulin is extremely hydrophilic and contains unusually high numbers of lysine, arginine, and asparagine residues. The carboxyl-terminal half of amphiregulin (residues 46 to 84) exhibits striking homology to the epidermal growth factor (EGF) family of proteins. Amphiregulin binds to the EGF receptor but not as well as EGF does. Amphiregulin fully supplants the requirement for EGF or transforming growth factor–α in murine keratinocyte growth, but it is a much weaker growth stimulator in other cell systems.

THE LIST OF PEPTIDE GROWTH REGulators has been expanding rapidly. These factors participate in various physiological and pathological conditions, such as cellular communication, growth and development, embryogenesis, immune response, hematopoiesis, cell survival and differentiation, inflammation, tissue repair and remodeling, atherosclerosis, and cancer (*1*). The isolation, characterization, and mechanism of action of regulatory factors for growth and differentiation are of current interest because of the potential use of such regulatory factors in the diagnosis, prognosis, and therapy of neoplasia and because of what these factors reveal about the basic mechanism of normal cellular proliferation and the unrestrained growth of cancer cells. We have recently reported the isolation of a novel glycoprotein termed amphiregulin (AR), which inhibits growth of A431 human epidermoid carcinoma and other human tumor cells and stimulates proliferation of human fibroblasts and other normal and tumor cells (*2*). AR was isolated from serum-free conditioned medium of MCF-7 human breast carcinoma cells that had been treated with 12-*O*-tetradecanoylphorbol-13-acetate (*2*). We now report the complete amino acid sequence of amphiregulin and compare its biological properties with those of the other members of the epidermal growth factor (EGF) family proteins.

AR was purified to homogeneity as described (*2*). The homogeneous AR was used for all the chemical and biological studies reported here. The amino acid sequence of human AR (Fig. 1) was determined by automated Edman degradation of *N*-glycanase–treated, reduced, and *S*-pyridylethylated AR (NG-SPE-AR) and of peptide fragments obtained by cleavage of NG-SPE-AR with various endopeptidases. The carboxyl-terminal analysis of NG-SPE-AR was performed with carboxypeptidase P (*Penicillium janthinellum*). The amino-terminal analysis of NG-SPE-AR revealed the presence of two sequences, one starting at residue 1, serine, and the other starting at residue 7, valine (Fig. 1). The yield of the larger form of AR was about 20% of that of the truncated form. The larger AR thus contains six additional amino acids at the amino terminal of the truncated form of AR. The larger form of AR and the truncated AR are single chain polypeptides of 84 and 78 residues, with a calculated molecular weight of 9759 and 9060, respectively (Fig. 1). Both forms of AR have a similar carboxyl-terminal sequence as determined by carboxypeptidase P cleavage (Fig. 1), and both are biologically active.

The sequence of AR was compared with all proteins in the National Biomedical Research Foundation database (release 15, containing 6796 protein sequences), Genetic Sequence Data Bank (Bolt Beranek and Newman, Los Alamos National Laboratory; release 54) and the European Molecular Biology Laboratory DNA sequence library (release 13). These computer-aided searches revealed that AR is a novel protein and a member of the EGF family. This family includes EGF (mouse, human, and rat) (*3–5*), transforming growth factor–α (TGF-α) (*6, 7*), and poxvirus growth factors [vaccinia (VGF), myxoma (MGF), and Shope fibroma (SFGF)] (*8–10*). Tissue-type plasminogen activator (*11*), the mammalian clotting factors IX and X (*12*), the low-density lipoprotein receptor (*13*), bovine protein C (*14*), human proteoglycan core protein (*15*), product of *Drosophila notch* gene (*16*), product of *lin 12* gene (*17*), the product of cell lineage–specific gene of sea urchin *Strongylocentrotus purpuratus* (*18*), cytotactin (*19*), and product of *Pfs* gene of *Plasmodium falciparum* (*20*) also contain EGF-like domains. Alignment of AR structure with the structure of EGF-like growth factors and with other members of EGF-like proteins (Fig. 2) reveals that AR, like other members of the family, contains the hallmark six essential cysteine residues, maintains conservation of cysteine residue spacing in the pattern $CX_7CX_4CX_{10}CX_1CX_8C$, and also contains some of the characteristic and conserved amino acids. AR falls between the members of the growth factor family that look like EGF and TGF-α and those that look like the poxvirus-encoded growth factors (MGF and SFGF), especially in the use of asparagine. The amino-terminal sequence of AR has some analogy with the amino-terminal sequences of the TGF-α's (*6, 7*), VGF (*8*), and MGF (*9*) in that it is rich in prolines, serines, and threonines and, like TGF-α and VGF, has potential N-linked glycosylation sites as well as the possibility for O-linked glycosylation in the region rich in serines, threonines, and prolines. Unlike MGF and SFGF, AR does not have any potential glycosylation site within the growth factor domain of the molecule. On the basis of homology with mouse EGF (*3*) and perfect alignment of six cysteine residues, one would expect the pres-

Oncogen, 3005 First Avenue, Seattle, WA 98121.